

# **Process Analytical Technology Case Study, Part I: Feasibility Studies for Quantitative NIR Method Development**

Robert P. Cogdill<sup>1</sup>, Carl A. Anderson<sup>1</sup>, Miriam Delgado-Lopez<sup>1</sup>, David Molseed<sup>1</sup>, Robert Chisholm<sup>2</sup>, Raymond Bolton<sup>2</sup>, Thorsten Herkert<sup>3</sup>, Ali M. Afnán<sup>4</sup>, James K. Drennen, III<sup>1, 5</sup>

<sup>1</sup>Duquesne University Center for Pharmaceutical Technology, <sup>2</sup>AstraZeneca, <sup>3</sup>AstraZeneca GmbH, <sup>4</sup>United States Food and Drug Administration, Center for Drug Evaluation and Research, Office of Pharmaceutical Science (Formerly of AstraZeneca), <sup>5</sup>Correspondng Author

“The views presented in this article do not necessarily reflect those of the Food and Drug Administration.”

## **Abstract**

This paper is the first of a series of articles detailing the development of NIR methods for solid dosage form analysis. Experiments were conducted at the Duquesne University Center for Pharmaceutical Technology (DCPT) to qualify the capabilities of instrumentation and sample handling systems, evaluate the potential effect of one source of a process signature on calibration development, and compare the utility of reflection and transmission data collection methods. A database of 572 production-scale sample spectra was used to evaluate the inter-batch spectral variability of samples produced under routine manufacturing conditions. A second database of 540 spectra from samples produced under various compression conditions was analyzed to determine the feasibility of pooling spectral data acquired from samples produced at diverse scales. Instrument qualification tests were performed, and appropriate limits for instrument performance were established. To evaluate the repeatability of the sample positioning system, multiple measurements of a single tablet were collected. With the application of appropriate spectral preprocessing techniques, sample repositioning error was found to be insignificant with respect to NIR analyses of product quality attributes. Sample shielding was demonstrated to be unnecessary for transmission analyses. A process signature was identified in the reflection data. Further tests demonstrated that the process signature was largely orthogonal to spectral variation due to hardness. Principal component analysis of the compression sample set data demonstrated the potential for quantitative model development. For the data sets studied, reflection analysis was demonstrated to be more robust than transmission analysis.

© AAPS PharmSciTech. Accepted: February 2, 2004.  
Author's final version.

Keyword: Process Analytical Technology, PAT, Near-Infrared Spectroscopy, NIR,  
Chemometrics, Tablet Analysis, Multivariate Analysis, Pharmaceutical Analysis, Hardness,  
Reflection, Transmission, Process Signature, Process Control

## Introduction

Process Analytical Technology (PAT) is defined by the United States Food and Drug Administration (FDA) in the document “Guidance for Industry: PAT – A Framework for Innovative Pharmaceutical Manufacturing and Quality Assurance” as “a system for designing, analyzing, and controlling manufacturing through timely measurements (i.e., during processing) of critical quality and performance attributes of raw and in-process materials and processes with the goal of ensuring final product quality.”<sup>1</sup> This is in contrast to the current practice of process validation whereby processes which are successfully operated in a repeatable manner (generally accepted as three consecutive successful batches) are accepted as validated. The current interpretation of cGMPs has been effective in providing the American consumer with the highest quality pharmaceutical products in the world. However, this interpretation has discouraged innovation in pharmaceutical manufacturing for three decades.

An element of the August 2002 FDA initiative “Pharmaceutical cGMPs for the 21<sup>st</sup> Century: A Risk-Based Approach,”<sup>2</sup> is a new scientific, risk-based framework that encourages the voluntary development and implementation of innovative pharmaceutical manufacturing and quality assurance. This framework is outlined in the PAT draft guidance released by FDA’s Center for Drug Evaluation and Research.<sup>1</sup> One of the potential outcomes from the implementation of PAT is the replacement of conventional quality assurance/quality control methods for product release with a new approach, termed *Real-time Release* (RTR). Real-time Release is a system that ensures a product is of the intended quality, while reducing or eliminating traditional end-product testing. PAT methods, including monitoring and control of process parameters, provide a platform for RTR.<sup>1</sup>

Advances in analytical technology provide the opportunity to develop a “Total quality management system” (TQMS) for implementation of PAT in a working manufacturing facility. A TQMS has the potential to provide significant improvements in product quality and manufacturing efficiency. Statistical confidence in decisions regarding product quality is enhanced by the TQMS because orders of magnitude more samples are analyzed, improving statistical power of the decisions. Further, the possibility of real-time data collection enables feedback mechanisms for control of the pharmaceutical manufacturing process.

Important elements of this TQMS include near-infrared sensors, a protocol for process control, and an integrated information management structure. Such a system provides a means of developing a higher level of process understanding. The TQMS has been implemented for an existing product for which production will be transferred to a new facility. The TQMS includes process monitoring and control systems and end product testing. This paper is the first of a series of articles detailing the development of NIR methods for solid dosage form analysis.

The first paper describes feasibility studies to verify the performance of an on-line tablet analyzer and provide data for calibration development. The second paper in the series will describe the development and validation of quantitative NIR calibrations for tablet API content and hardness, including the selection and optimization of chemometric techniques. Paper number three will illustrate the philosophy and methodology of implementing and managing calibrations to ensure the continuity of performance, including a detailed description of performance monitoring and calibration transfer techniques. The experimental results to be covered in this series will show that, for this application, a properly-developed NIR method provides predictive analyses which are comparable to the accuracy of the reference methods currently employed, while reducing the time and cost of analysis.

NIR spectroscopy is an important component of a PAT toolbox, and is a key technology for enabling RTR of pharmaceutical tablets. NIR spectroscopy has gained wide acceptance in the agricultural, food, and petrochemical industries as a powerful analytical technique since its early development as a means of rapidly analyzing the quality of agricultural commodities.<sup>3</sup> NIR is capable of rapid on-line and in-line analyses of a diverse array of products and materials.<sup>4</sup>

Recently, NIR spectroscopy has found increasing use in pharmaceutical analysis for identification and quality testing of raw materials,<sup>5, 6</sup> monitoring of blending,<sup>7-9</sup> granulation,<sup>10, 11</sup> roller compaction,<sup>12</sup> and drying operations,<sup>13</sup> and many other applications.<sup>14, 15</sup> One of the most promising pharmaceutical applications of NIR spectroscopy is the analysis of solid oral dosage forms. NIR spectra are rich in chemical and physical information. When used in conjunction with appropriate chemometric modeling techniques (multivariate analyses),<sup>16-18</sup> NIR spectroscopy can be used to measure a variety of tablet properties. NIR is effective in transmission or reflection modes as a noninvasive and nondestructive technique for the simultaneous measurement of a variety of tablet properties.<sup>19-23</sup>

Numerous wavelength modulation technologies are available for NIR spectrometry.<sup>4, 24</sup> While each technology has its own strengths and weaknesses, acousto-optic tunable filter (AOTF) technology was chosen for this work because of its combination of fast data acquisition rate, dual-channel detection (double-beam in-space<sup>24</sup>), and lack of moving parts.

## Objectives

While much of the theory behind reflection and transmission analysis of solid pharmaceutical tablets using NIR spectroscopy is well understood,<sup>20</sup> a number of practical investigations are required during the early stages of developing a NIR spectroscopic method. The objectives of this work were to:

- I. Qualify capabilities of the instrument and the sample handling system.
- II. Evaluate the potential effect of one source of a process signature on calibration development.
- III. Compare the utility of reflection and transmission data collection methods.

## **Materials and Methods**

### **NIR Instrumentation**

A Brimrose, Luminar 3070 (Brimrose Corp., Baltimore, MD) double-beam scanning AOTF spectrometer was used for this work. The spectrometer is tunable across the range of 900 – 2300 nm, and is integrated with the sample transport/presentation system. The tablet analyzer system consists of an enclosed light source, AOTF, reference detector, a reflection detector situated above the tablet conveyor belts, and a remote transmission detector placed in the field of view (FOV) beneath the tablet conveyor belts. The reflection and transmission detectors are aligned with the source illumination so that both reflection and transmission spectra can be acquired without repositioning of the sample.

AOTF spectrometers are unique in their method of wavelength modulation, which is based on the acoustic diffraction of light in an anisotropic medium. The device consists of a piezoelectric transducer bonded to a birefringent TeO<sub>2</sub> crystal. When the transducer is excited by an applied RF signal, acoustic waves are generated in the crystal. The propagating acoustic waves produce a periodic modulation of the refractive index, causing the crystal medium to become a moving transmission grating with “refractive index grooves” of spacing equal to the acoustic wavelength in the medium. For a fixed acoustic frequency, a narrow band of optical frequencies satisfy the phase matching conditions, and are cumulatively diffracted.

Thus, by scanning the transducer across a range of RF frequencies, a continuous NIR spectrum can be obtained. Light transmitted through and AOTF is split into two beams, the ordinary and extraordinary rays, according to the polarization of the beam. This is advantageous because an optical transducer can be placed in the path of the unused beam to act as a double-beam reference detector, which has significant benefits in terms of stability and signal-to-noise ratio (SNR).

NIR spectrometers should be subjected to a thorough series of performance tests to ensure the quality and consistency of analyses derived from the spectra before being used in the collection of spectral data, and at specific periodic intervals. Two performance test protocols were utilized for this work, including an internal performance test for continuous instrument monitoring and predictive maintenance, and an external performance test to be used for periodic (e.g.- semi-annual, or following instrument maintenance operations) qualification of instrument performance.

The internal noise test consists of a series of built-in diagnostic functions (which can be performed autonomously as defined by an operational protocol), including tests for wavelength accuracy, wavelength repeatability, reference detector noise, and a survey of internal diagnostics sensors. The internal wavelength accuracy and repeatability tests are performed by analyzing the spectral features of a polystyrene filter inserted in the reference detector optical path (by an electrical actuator). Since there is no internal means to measure sample detector noise (e.g.- by automatically placing a reference standard in the FOV), sample channel noise is monitored continuously by analyzing the high-frequency components of every sample spectrum acquired. By examining the trend of internal performance test scores, instrumental drift (e.g.- lamp aging) or failure can be readily detected.

The purpose of external performance testing is to monitor the performance of the instrument with respect to a set of certified, traceable reference standards. Moreover, the external instrument performance test offers a more detailed record of instrument condition, and a redundant check of instrument performance following major instrument repairs (e.g.- lamp replacement). The external performance test is designed in accordance with U.S.P. recommendations,<sup>25</sup> and allows for testing wavelength accuracy, absorbance linearity, and high/low flux instrumental noise. These tests demonstrate continuity of process analyzer performance, rather than absolute correlation with the certified analysis of reference standards. External performance evaluation is designed to establish a baseline for instrument performance during method implementation and subsequent quantitative analyses.

The external performance test was performed in reflection mode, twice daily, over a period of 40 days to evaluate both the instrument performance and the external performance testing protocol. For the wavelength accuracy test, the precise location of major peaks in the spectra of

NIST SRM-1920A were measured; peak centers were found by locating the zero-crossing in the 1<sup>st</sup> derivative of the quadratic equation fit to the data points of each major peak (Figure 1).

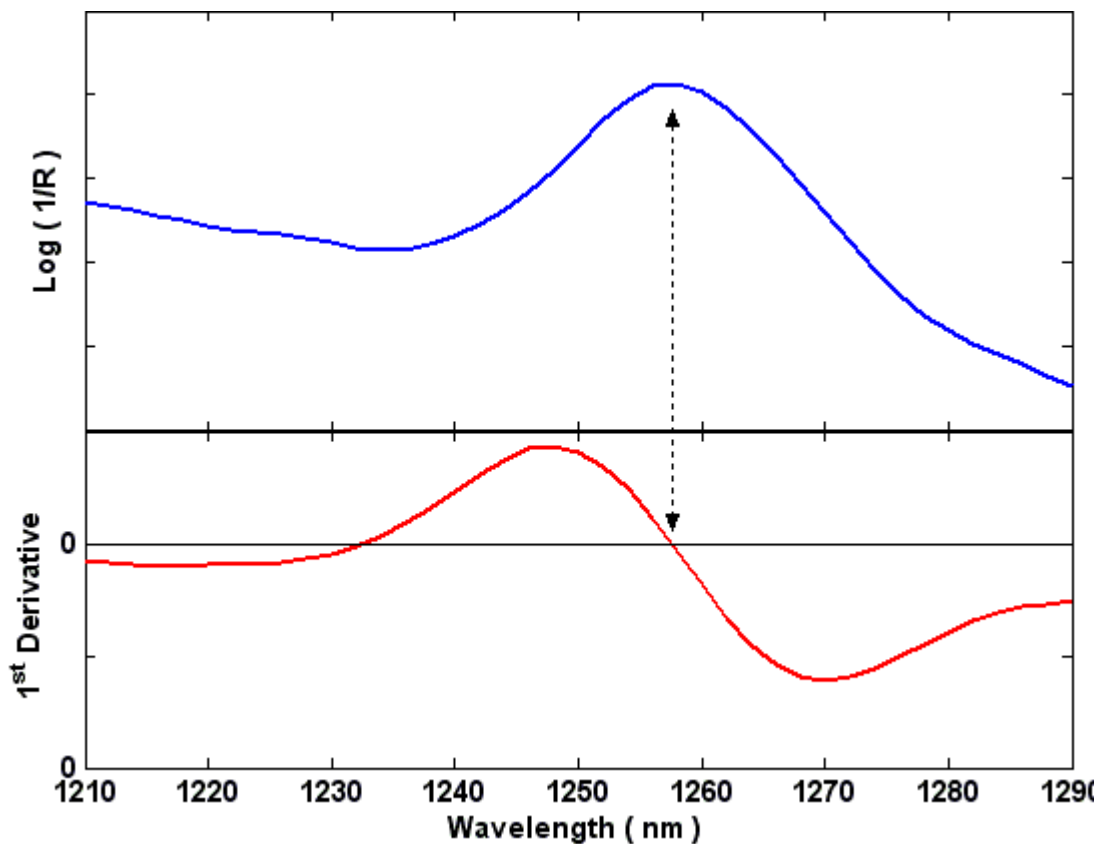
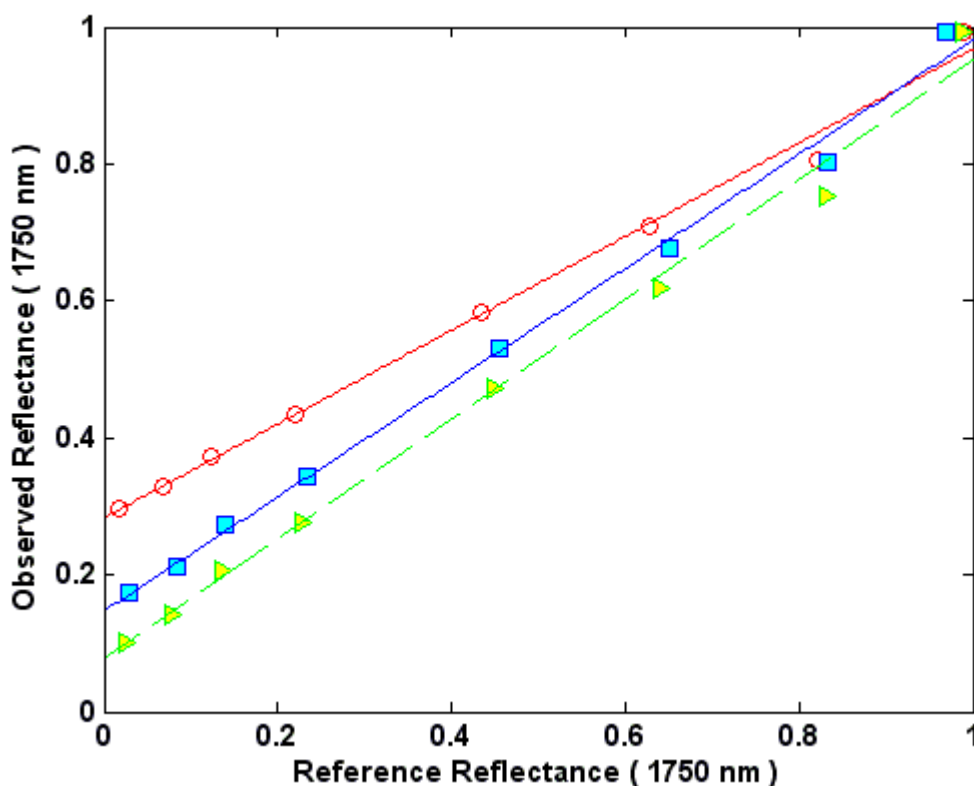


Figure 1. Wavelength axis accuracy measurement. The center of major peaks in the absorbance spectrum of a wavelength standard (upper curve) are located by calculating the zero crossing of the first derivative (lower curve) of a windowed quadratic fit of the spectrum.

The absorbance linearity test was performed by measuring the reflection of a series of eight standards (99, 80, 60, 40, 20, 10, 5, and 2% nominal reflection). Linearity was calculated by regression of the observed reflection at 1200, 1600, and 2000 nm against a set of certified reference reflection values (Figure 2). High- and low-flux spectrophotometer noise were calculated by measuring the root mean square (RMS) variation in  $\log(1/R)$  intensity for repeated scans of the 99 and 10% reflection standards, respectively. Each standard was scanned 64 times (without replacement), and converted to absorbance ( $\log 1/R$ ); RMS variation was calculated in successive 100-nm segments across the length of the spectrum. While the external performance test outlined above utilized reflection measurements, the same tests can be performed in transmission mode by substituting the reflection standards with a suitable set of transmission standards.



**Figure 2. Reflectance linearity testing using certified reflectance standards at 1200 (circles), 1600 (triangles), and 2000 nm (squares).**

### **Sample Transport System**

A custom-made tablet transport system was designed specifically for this application to position sampled tablets for spectroscopic measurements. Besides having suitable sample acquisition speed, the system was designed to operate autonomously and within the potent compound containment area. The sample transport conveyor consists of two flat belts running in parallel, with tablets placed straddling the center of both belts; there is a narrow gap between the belts to allow transmitted NIR radiation to be collected by the detector placed underneath the belts. Once the tablets are placed on the sample transport conveyor, a series of stationary guide rails precisely center the tablets. A laser diode and detector sense when a tablet has reached the field of view (FOV) of the NIR analyzer. When a tablet crosses the laser beam, a trigger signal is sent to the analyzer control computer to stop the belt and activate the analyzer. Since there is a lag time between the interruption of the laser beam and the termination of conveyor motion (due to inertia and computational delays), the position sensor is placed slightly ahead of the FOV, and an adjustable delay is used between the trigger pulse and the commencement of NIR analysis. Following NIR analysis, the tablets are routed to other instruments for further analyses, and are ultimately retained in blister packs for parallel off-line testing.

An experiment was conducted to determine the ability of the sample transport system to repeatedly position tablets within the spectrometer FOV. A single 50 mg tablet (6.5 mm diameter) was manually dropped 34 times onto the sample transport conveyor ahead of the centering guide rails, and was automatically positioned for analysis using the system described above.

Reflection and transmission spectra were collected each time the tablet was positioned within the spectrometer FOV, while a machine vision camera was used to precisely measure the position of the tablet along the conveyor belts (within 0.4 mm). The effect of sample repositioning was compared for reflection and transmission analysis.

A series of tests were conducted to determine the need for tablet shielding during transmission analysis. NIR spectra of tablets were measured with and without shielding and the spectra were compared. Shielding consisted of an aperture (3-mm) placed between the sample and the detector.

### **Production and Compression Samples**

Tests were conducted to determine the level of inter-batch spectral variation, and the feasibility of pooling spectral data from multiple production- and laboratory-scale batches for development of a calibration database. Another goal of these feasibility studies was to decide whether to develop the method using transmission or reflection data. Two sets of tablets were available for these experiments, defined below as *production* samples and *compression* samples.

The purpose of the first sample set, production samples, was to evaluate the typical batch-to-batch spectral variability of tablets manufactured at production-scale. The production set consisted of 572 unique tablet samples drawn from each of thirteen different lots of 50-mg tablets (44 tablets per batch) manufactured over the course of approximately one year and selected to provide maximum variability in potency and hardness, as determined from batch records.

Each tablet was scanned once in both the reflection and transmission modes. In addition to the spectral analyses, single-tablet measurements of potency or hardness were performed using off-line reference techniques. The tablets analyzed for potency ( $n = 130$ ) were tested using HPLC with UV detection. The mean and standard deviation of potency were 50.1 and 2.7 mg, respectively. Hardness ( $n = 128$ ) was measured using the diametral crushing strength test. The mean and standard deviation of hardness were 70.0 and 11.2 N, respectively.

The second sample set, or compression samples, consisted of 540 tablets, where samples of granulate were drawn from production-scale batches, and compressed using one of three different scales of tablet press (single-punch, small-scale rotary, or large-scale rotary). As described above, each tablet was scanned once in both the reflection and transmission modes. The actual hardness of each tablet was measured using the diametral crushing strength test. The mean and standard deviation of tablet hardness were 72.3 and 33.4 N, respectively. The purpose of the multi-scale compression test was to determine whether or not spectral data from both laboratory- and production-scale samples could be pooled for calibration development. Laboratory-scale samples were required to expand the range of API and hardness values beyond the variability found in samples produced during routine manufacturing.

The production and compression spectral datasets were analyzed using principal component analysis (PCA). All data analyses were performed using Matlab 6.5 (The Mathworks, Natick, MA), and the PLS Toolbox 3.0 (Eigenvector Research, Inc., Manson, WA). All data analysis was performed at the Duquesne University Center for Pharmaceutical Technology (DCPT).

## **Results and Discussion**

### **Instrument Qualification Testing**

Qualification of instruments used in this study was performed to demonstrate the suitability of the instrument for data collection using regularly scheduled internal and external performance test protocols. Internal performance tests were conducted daily to demonstrate that the instrument was operating within the manufacturer's recommended specifications. Because the U.S.P. noise test requires external standards not easily placed in the beam path, a sample-based noise test was developed. This test, based on analysis of every sample spectrum, will be described in detail in the third paper of this series. Instrument performance control limits were set as  $\pm 0.5$  nm wavelength accuracy, 10 and 30 mAU mean low- and high-flux noise, respectively, and variation in linearity slope and intercept should not exceed  $\pm 0.25$  and  $\pm 0.1$ , respectively.

While the U.S.P. external instrument performance test method suggests control limits for each of the performance tests, it is appropriate to specify control limits that are relevant to the performance requirements of the analytical application and the capabilities of the instrumentation. Subjecting PAT methods to arbitrarily strict specifications will not improve performance, but will ultimately lead to delays stemming from routine instrumental variability. Initial limits for external performance testing were set based on the variations experienced during the external performance testing during data collection for method development.

### **Automatic Positioning and Shielding Tests**

Out of 34 re-scans of a production-scale tablet, four transmission spectra were observed to be atypical, while three of the reflection spectra were observed to be atypical (Figure 3 & Figure 4). Note that the reflection and transmission scans are recorded without replacement. The atypical scans were not due to variation in linear positioning of the tablet, but were the result of tablet orientation problems. The tablets were stuck vertically between the tablet conveyor belts. While such major positioning errors are easily detected, so the analysis can be aborted, the frequency of occurrence required investigation. One of the four atypical transmission spectra was paired with a viable reflection spectrum. This is an example of the comparative robustness of the reflection mode with respect to sample orientation. The results of this study allowed optimization of the conveyor system and demonstrated an advantage of the reflection mode. Following adjustments, the failure rate was reduced substantially. Further, the system is designed to capture, package and label all samples after NIR analysis, offering the ability to verify the cause of any atypical spectra. Such spectra are detected by a calibration monitoring system that will be discussed in subsequent installments of this series.<sup>26</sup>

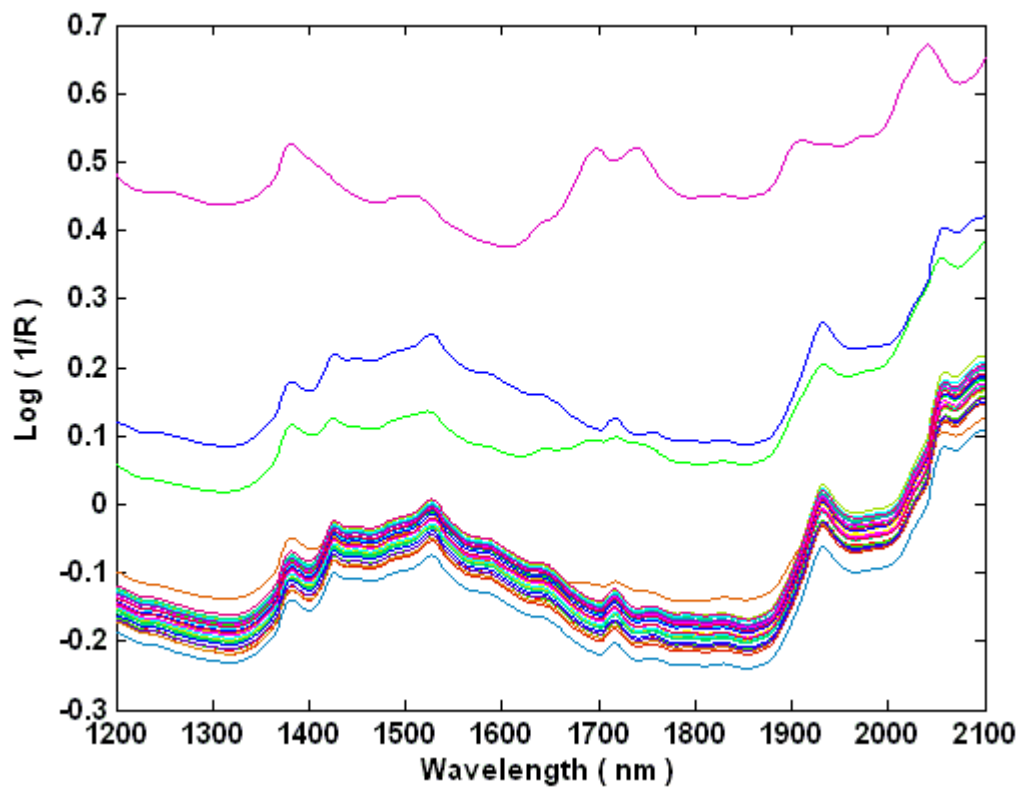


Figure 3. Single-tablet reflectance spectra with repeated positioning using an automatic tablet transport system. The three irregular spectra are the result of tablet mis-alignment on the transport conveyor belts.

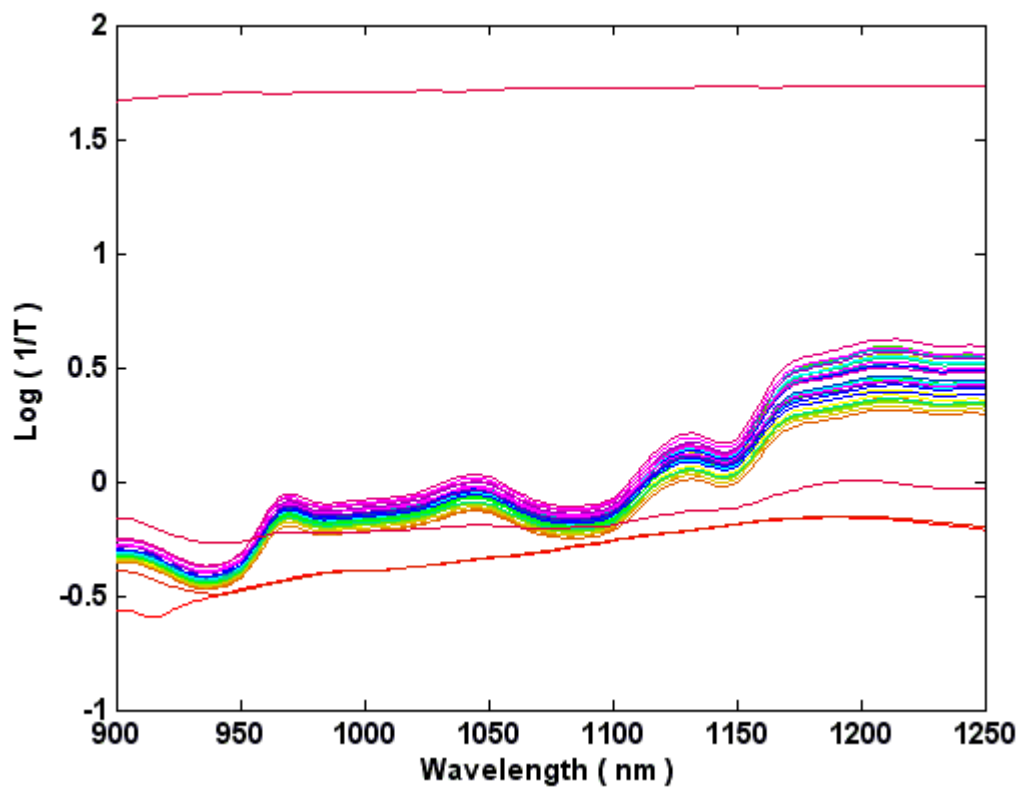


Figure 4. Single-tablet transmission spectra with repeated positioning using an automatic tablet transport system. The four irregular spectra are the result of tablet mis-alignment on the transport conveyor belts.

For the remaining 30 viable spectra, it was found that the automatic positioning system is capable of reproducing tablet position within approximately 0.96 mm. This translates to a standard deviation of 0.115 and 0.329 absorbance units for the raw reflection and transmission spectra, respectively. The bulk of spectral variation due to sample repositioning took the form of a change in spectral baseline, however, which is easily mitigated by a number of data preprocessing techniques, including the standard normal variate (SNV) transformation:<sup>17, 18</sup>

$$\hat{x} = \frac{x - \bar{x}}{\sigma_x} \quad (1)$$

Where:

$x$  = Vector of NIR absorbance intensities (e.g.- NIR spectrum)

$\hat{x}$  = SNV transformed vector of NIR absorbance intensities

$\bar{x}$  = Mean absorbance intensity for the current spectrum

$\sigma_x$  = Standard deviation of absorbance intensity for the current spectrum

After SNV transformation, the mean standard deviation of NIR absorbance intensity was reduced to 0.013 and 0.025 AU for the reflection and transmission spectra, respectively (spectra were re-scaled to original intensity scale). The SNV transformation is also useful in reducing other extraneous spectral variations such as instrumental baseline drift.

One drawback reported by some researchers for single-tablet NIR transmission analysis is the need to place a shield (mask, or aperture) in the beam path.<sup>27</sup> This is done so that light which has not penetrated the tablet, but rather has traveled around the surface of the tablet edge, will be blocked; while light that has traversed the entire cross-section of the tablet will be detected. Light which has been conducted around the surface of the tablet will have a much lower effective pathlength, and will have a nonlinear effect on absorbance spectra. It would be reasonable to expect, however, that instruments with a small illumination spot size (relative to tablet diameter, e.g., this AOTF spectrometer) will have less need for shielding. Furthermore, the geometrical relationship between the tablet and detector will also have some influence on the need for shielding.

The transmission shielding test spectra were analyzed and it was found that the spectral difference between scans (with and without shielding) is manifested as a simple baseline shift, which was easily rectified with SNV preprocessing. While other suitable and complementary preprocessing treatments are available,<sup>17, 18</sup> the SNV transformation is used exclusively for the remainder of this work because of its simplicity and ease of interpretability. Very little light is actually being transmitted through the tablets beyond 1150 nm. Consequently, the transmission spectra were truncated to include the range from 900 – 1150 nm for all further data analyses.

### **Production Sample Study**

The production-scale reflection and transmission spectra (SNV transformed) are shown in Figure 5 and Figure 6. A pronounced band of spectral variation can be seen in the reflection spectra, covering the range from 1430 – 1576 nm, centered near 1516 nm. Both the API and lactose have absorbance bands nearby at 1526 and 1530 nm, respectively (Table 1). However,

investigation of the spectral autocorrelation matrix reveals that the band is not correlated with any other features in the spectra (Figure 7).

**Table 1. NIR absorbance bands of major tablet constituents.**

Component	Bands (nm)									
API	968	1046	1130		1424	1526	1658	1716		2054
Lactose	904	1046	1094	1204	1276	1374	1530	1792	1932	2090
Na. Starch				1190	1466	1568		1768	1932	2096
Polypovidone				1176	1446	1550	1696	1726	1934	
Mg. stearate	916	1038		1206	1390	1418	1724	1758	1928	

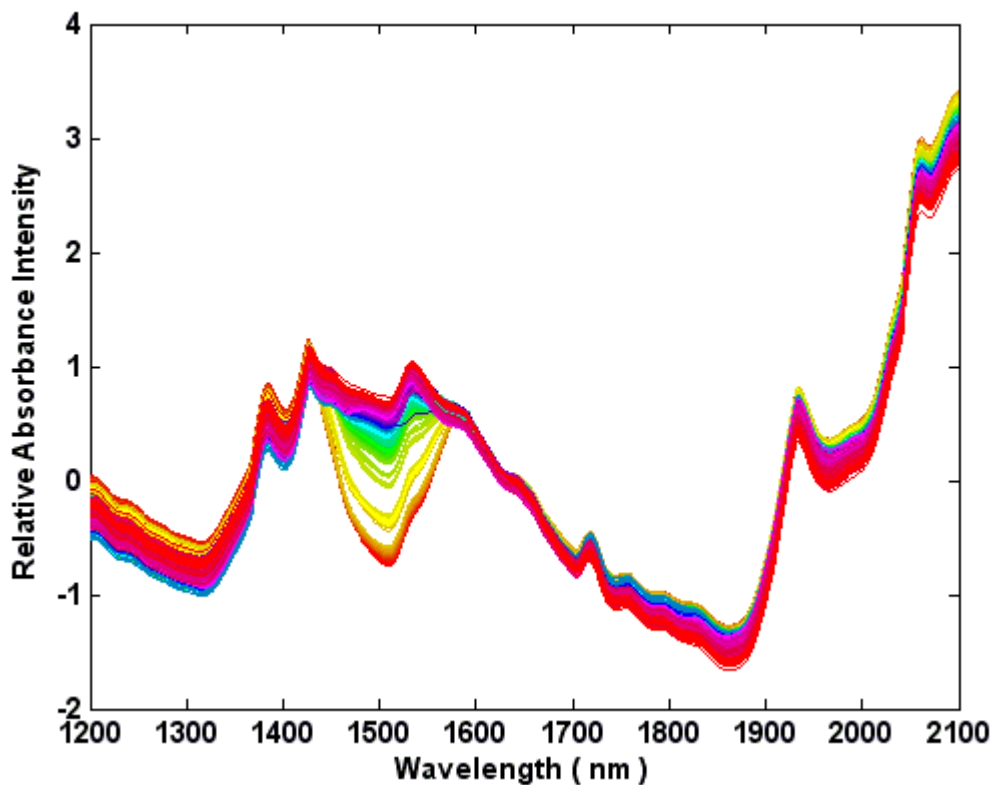


**Figure 5. Production sample reflection spectra after SNV pretreatment (N = 572).**

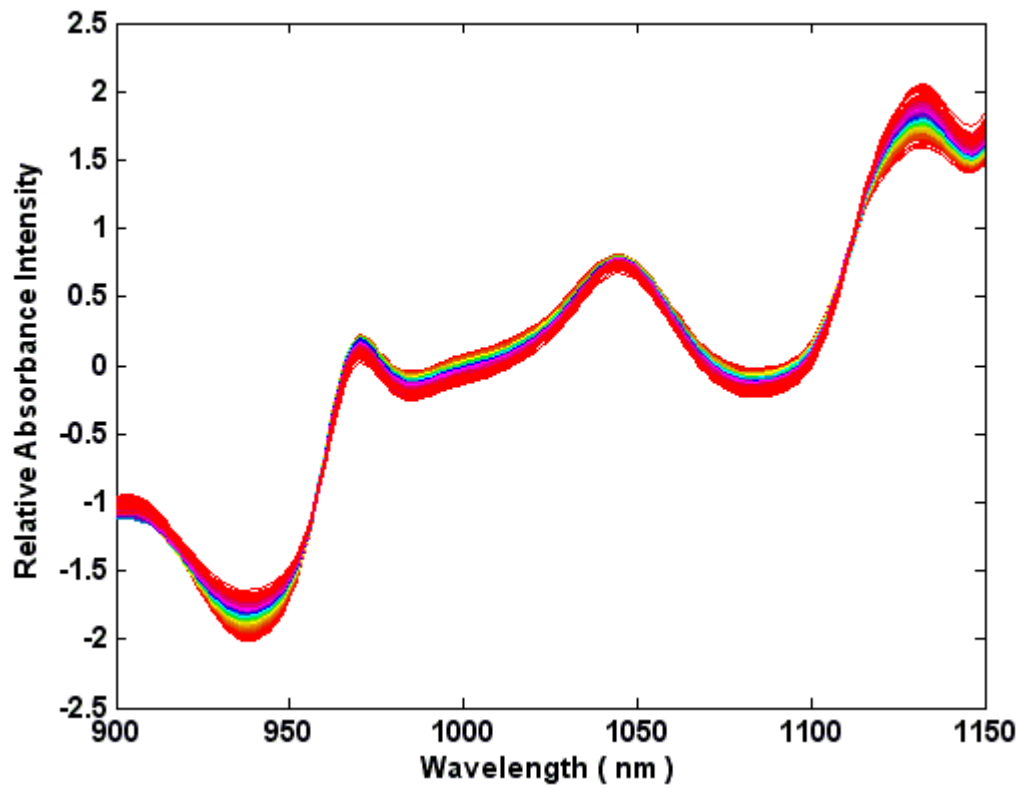
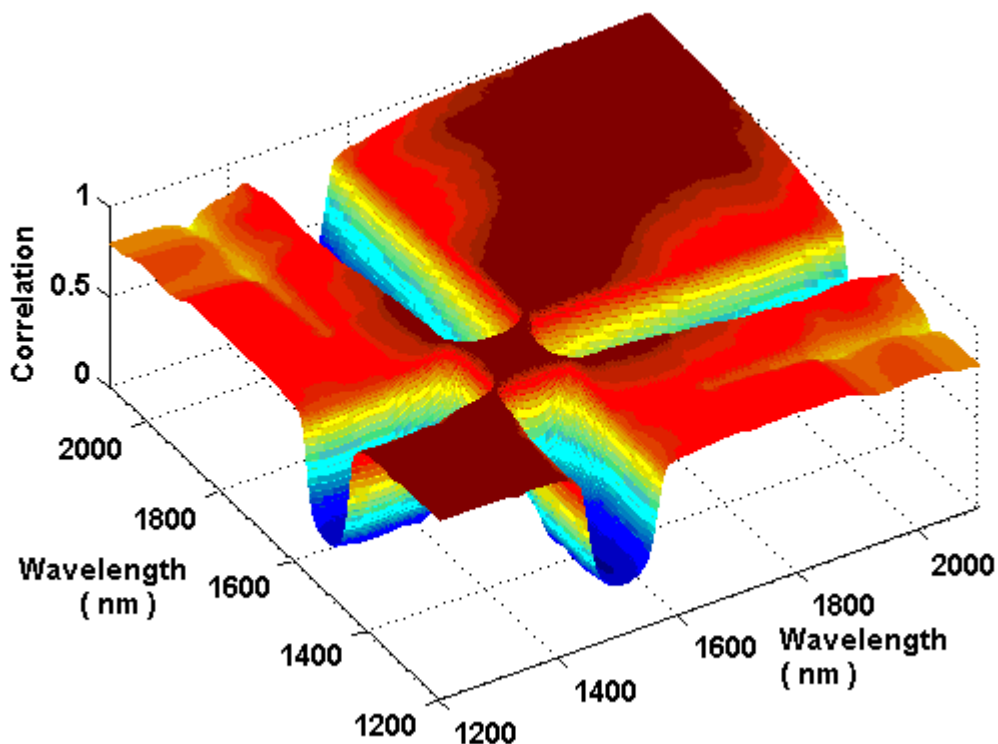


Figure 6. Production sample transmission spectra after SNV pretreatment (N = 572).



**Figure 7.** Surface plot of the autocorrelation matrix calculated using the raw production sample reflection spectra. The lack of correlation between the major band of variance centered at 1563 nm and any off-diagonal peaks suggests that the variation is not due to chemical changes in the samples, but is more likely an instrumental effect.

This suggests a localized instrumental effect. Furthermore, principal component analysis of the reflection spectra confirmed the dominating effect of this variation on the reflection spectra of production-scale tablets. The first principal component (PC), which explained nearly 84% of the total spectral variance had a single peak centered near 1516 nm. Thus, all further analyses were performed with the 1430 to 1576-nm band omitted.

PCA was performed on the spectra which were modified as described above. Two PCs explained >97% of the spectral variation. The principal component loadings and scores are

shown in (Figure 8 & Figure 9). The first PC loading vector (Figure 8) isn't easily interpreted, and is perhaps correlated to broad moisture absorbance effects, and to a lesser extent the API absorption band near 2054 nm. The second PC, however, appears to be correlated with lactose (Figure 8).

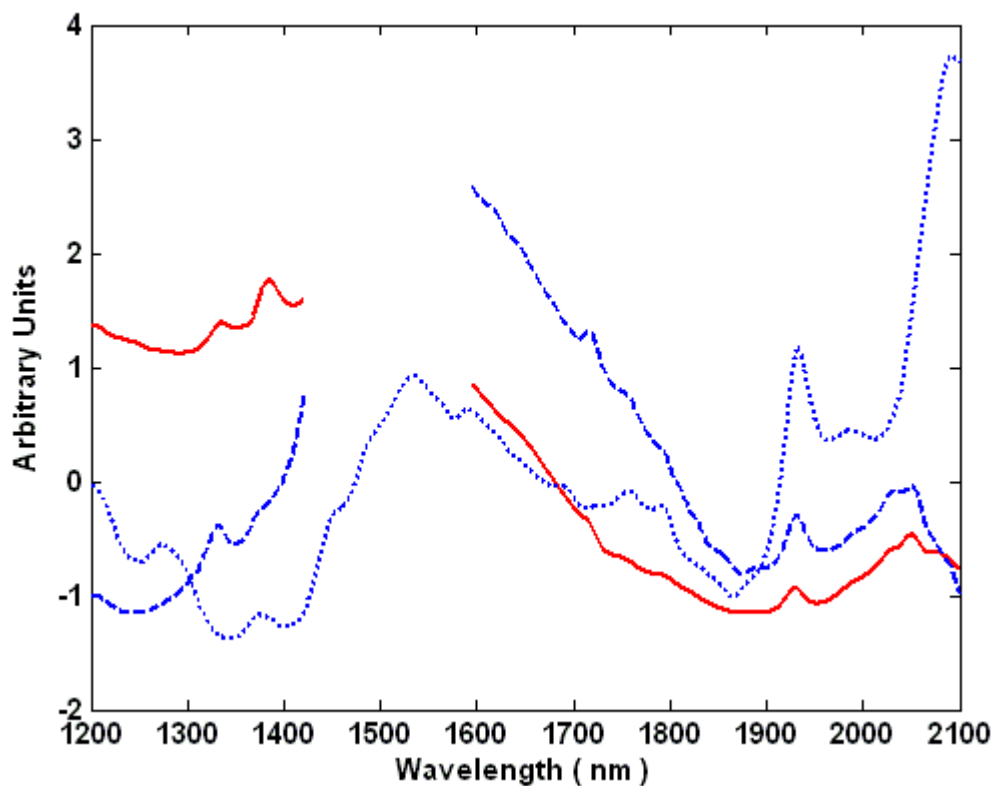


Figure 8. First two loading vectors from PCA of production samples and reflection spectrum of pure Lactose. PC 1 (solid line), PC 2 (dashed line), and Lactose (dotted line).

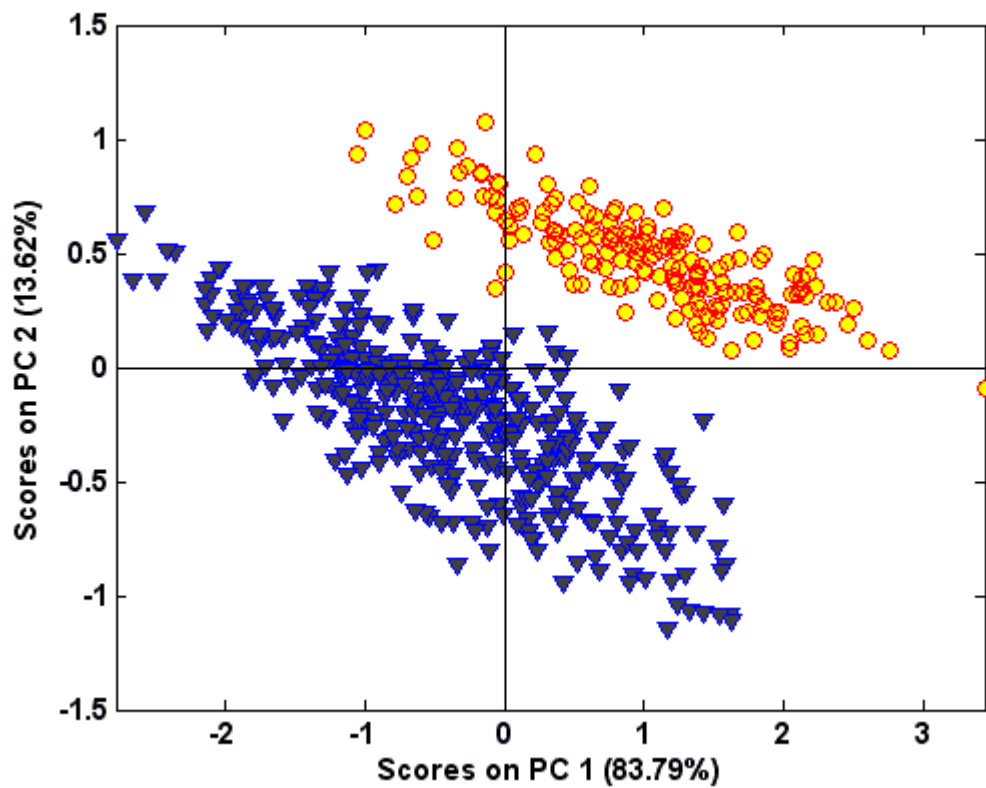


Figure 9. Scores plot of first and second principal components from PCA of production samples using reflection data.

The principal component score plot (Figure 9) reveals two data clusters, each representing multiple batches. The clustering is apparently due to the sensitivity of NIR spectroscopy to a *process signature*.<sup>1</sup> Process signature is defined as “A single or multi-dimensional signal indicative of the attributes of the process.”<sup>28</sup> It was observed during subsequent calibration development that the process signature did not impair the ability to predict product quality attributes such as hardness and API content.<sup>29</sup>

The PCA loadings and scores for the transmission spectra are shown in Figure 10 & Figure 11. The first PC, which explained nearly 88% of the spectral variance, appears to be mainly related to API content, with major peaks centered at 935, 1046, and 1132 nm (Table 1). The second and third PCs, which explain an additional 10% of the spectral variance, are likely related to excipient and moisture concentrations. The three-axis plot of the principal component scores does not show any significant clustering in the data, supporting the hypothesis that spectra from many production batches can be pooled for calibration development.

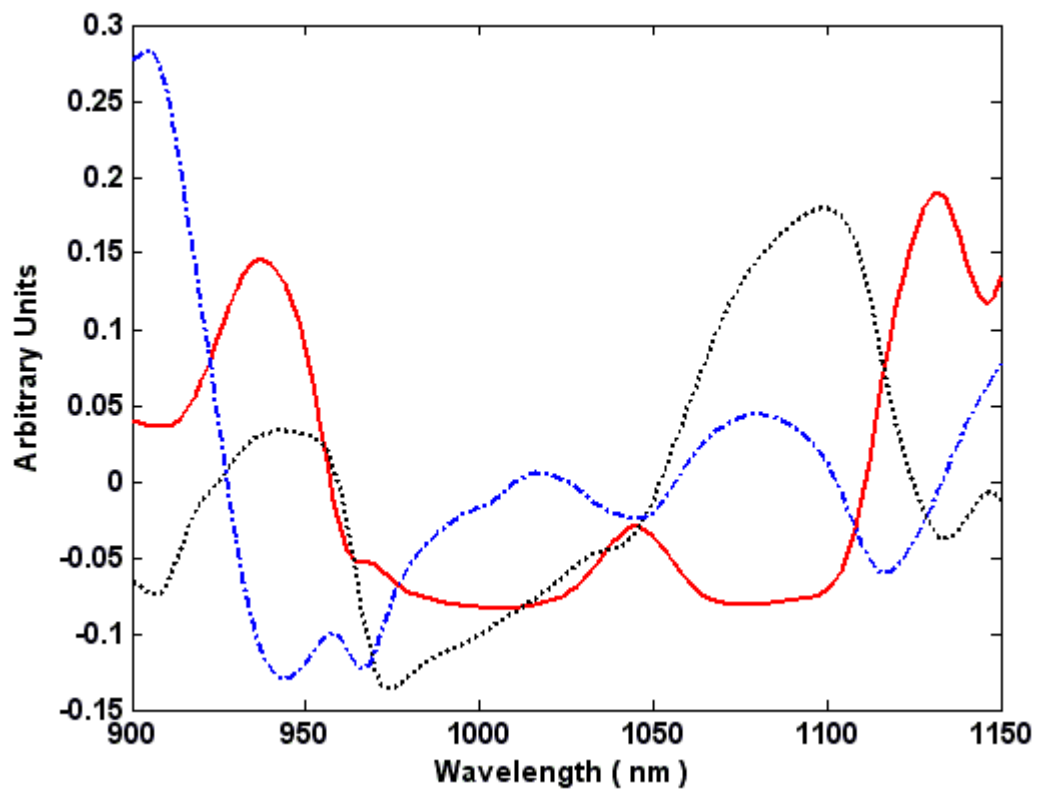
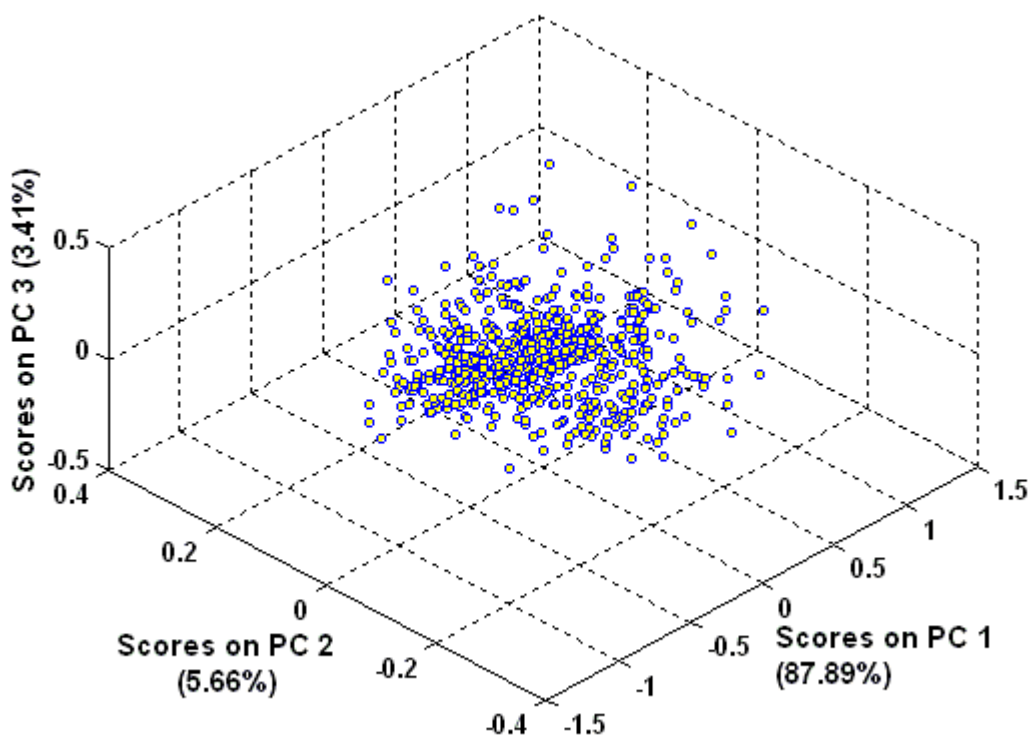


Figure 10. First three loading vectors from PCA of production sample transmission spectra. PC 1 (solid line), PC 2 (dash-dot line), and PC 3 (dotted line).



**Figure 11. Scores plot of first three principal components from PCA of transmission spectra of production samples.**

This is important because it will be necessary to pool production and compression data to achieve sufficient range for quantitative calibration development. For example, a NIR method for quantitative analysis of potency should have prediction error no larger than 25% of the total potency variation modeled.<sup>30</sup> The minimum error of prediction is limited by the standard error of the reference method (e.g., HPLC-UV). Thus, if the reference analytical technique used to measure API concentration has standard error of ~3%, the population of tablets used for calibration development must have a minimum of 12% standard deviation in potency. Regardless of the error of the reference method, the calibration range must span at least the product specification range (e.g.,  $\pm 10\%$  potency).

Finally, in order to build a suitable calibration for a single factor such as API content, other potential sources of variation must be included in the model. Examples for an API model may include hardness, the concentration of other tablet constituents, and the source of raw materials.

### **Compression Sample Study**

As demonstrated with production samples, the spectral region from 1430 to 1576 nm was omitted during the analysis of the compression test reflection spectra. A two-component PCA model captured nearly 99% of the spectral variation (Figure 12). The first PC, which explained nearly 98% of the variance, is related to tablet hardness. The coefficient of determination between the first PC and hardness was 0.92 (Figure 13). The second PC is a manifestation of the process signature between the single-punch and rotary tablet presses. The actual spectral features induced by the scale differences are subtle. PCA highlights the available variance in the spectra, as displayed in Figure 14. At first glance, this suggests that it would be inappropriate to pool such seemingly diverse spectral data from samples manufactured at different scales. However, since only two experimental factors were varied (compression force and equipment scale) while the remaining process variables were unchanged, the scale of manufacturing had high leverage on the PCA model. If other experimental conditions were varied, such as API content, the relative influence of process scale would be diminished. Furthermore, the effect of manufacturing scale was limited to a single PC, which was orthogonal to the first principal component (that was correlated with the effect of varying hardness). This indicates good potential for developing quantitative calibrations orthogonal to this process signature, providing sufficient net analyte signal for the quality parameter of interest remains. This illustrates that product quality parameters can be modeled despite the presence of manufacturing scale differences.

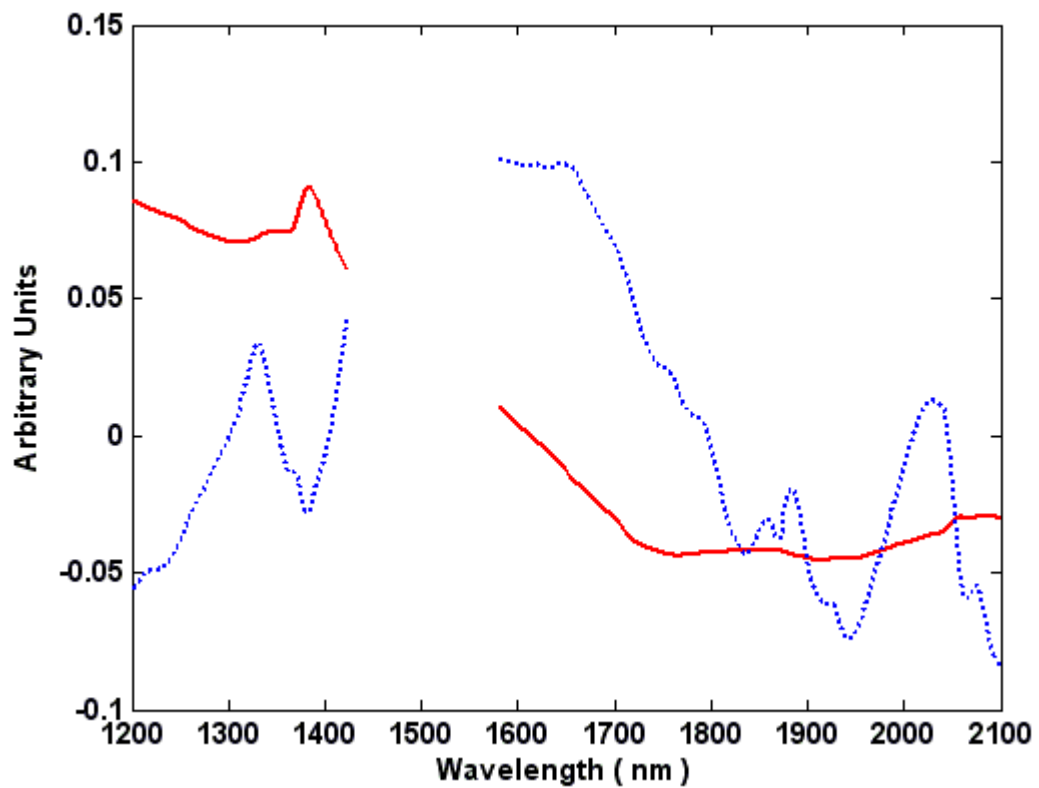


Figure 12. First two loading vectors from PCA of reflection spectra from compression samples. PC 1 (solid line), PC 2 (dotted line).

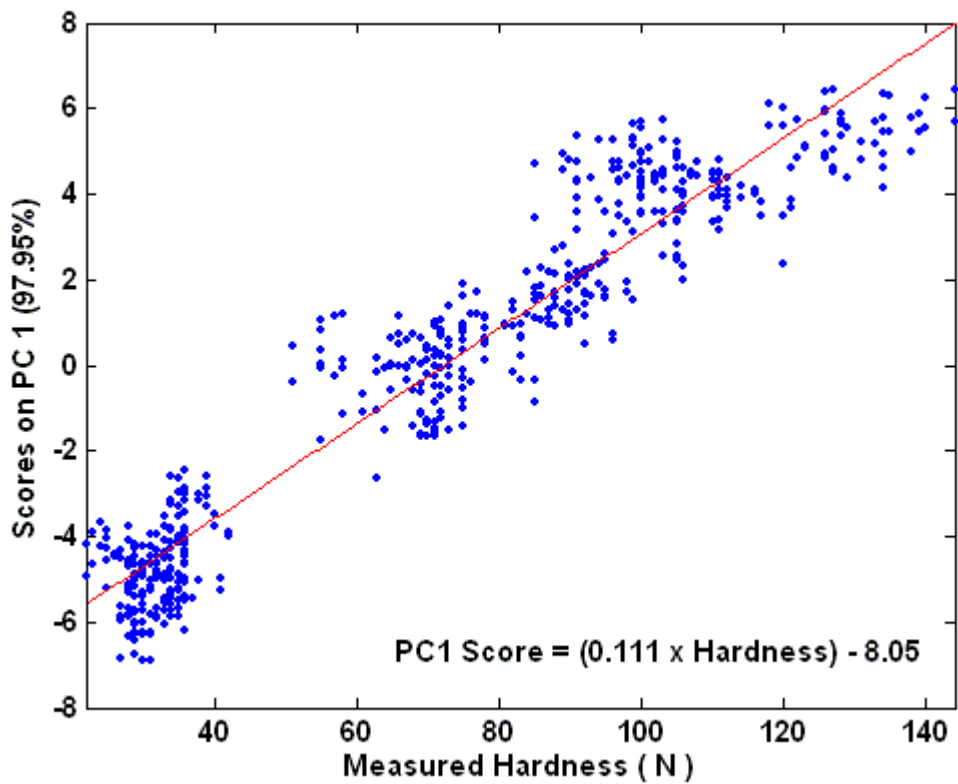
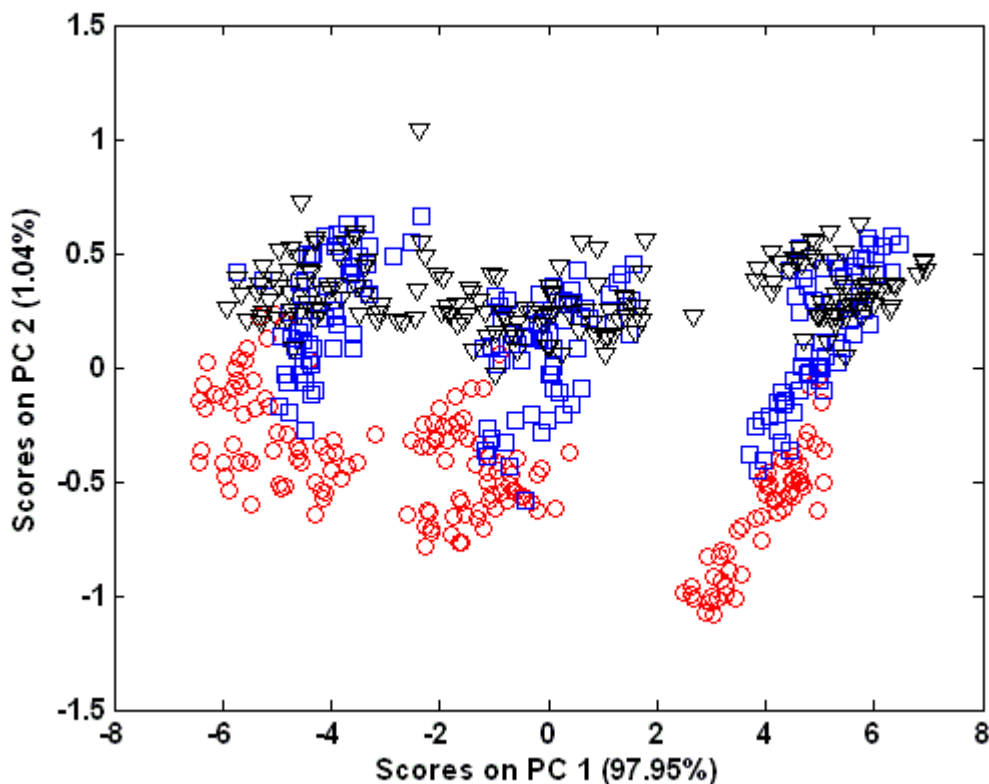


Figure 13. Correlation plot of measured tablet hardness against PC 1 score for compression sample reflectance spectra.



**Figure 14. Principal component scores plot from PCA of reflection spectra of compression samples. Single-punch tablet press = red circles, Small-scale rotary press = blue squares, Large rotary tablet press = black triangles.**

As an example, when the production sample study data are projected onto the PCA model from the compression sample study, the nature of the clusters in the production data is apparent. The two clusters which were observed in the scores of the production sample PCA model also appear in the projection of the production sample data onto the compression PCA model (Figure 15). The direction of segregation between the clusters is along the axis described by manufacturing scale, while the direction correlated to hardness does not show structure. This suggests that the nature of the clusters might be due to process signature. While many other

variations in the sample are feasible, the separation of the clusters lies in the same hyperspectral direction as the process signature observed in the compression study.

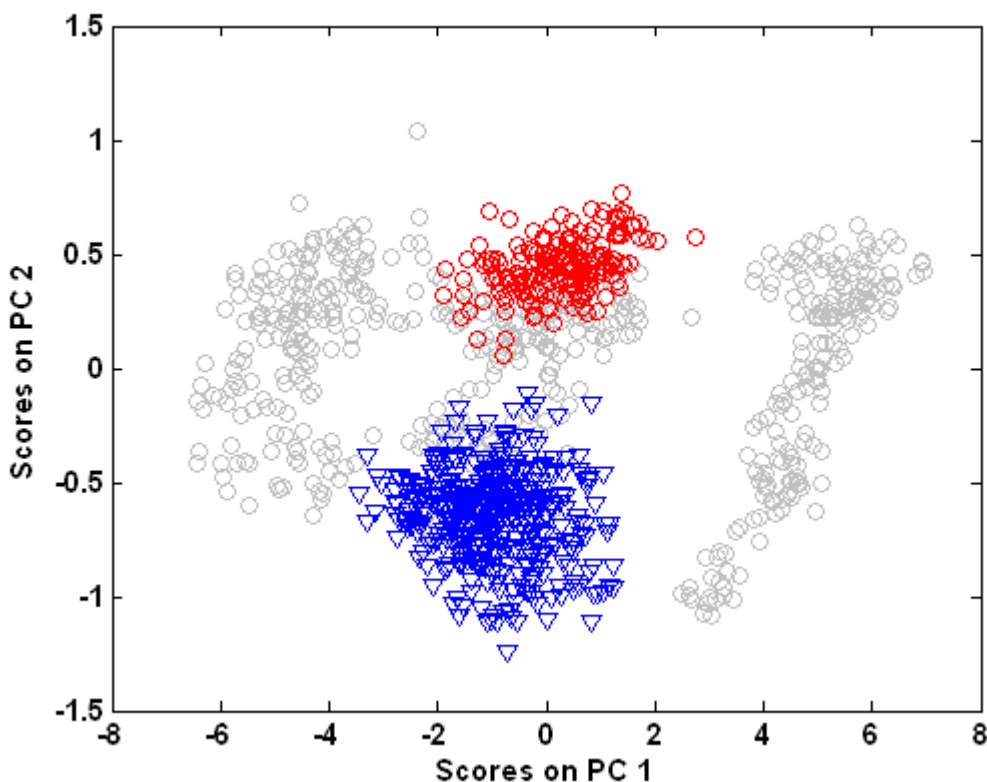


**Figure 15. Score plot of first and second PCs from projection of production sample reflection spectra onto the compression sample model. Note that PC1 correlates well with hardness while PC2 is indicative of process signature.**

A two-component PCA model explained over 98% of the transmission spectral variance. The first PC explained 95.4% of the spectral variance and 90.6% of the hardness variation (Figure 16). Unlike the reflection compression test model, the second PC of the transmission compression test model does not appear to be related to process scale, nor is it correlated to hardness (Figure 17). The correlation with hardness of both the reflection and transmission

models confirm that spectral data from tablets manufactured across a range of production scales can be pooled for quantitative regression model development.

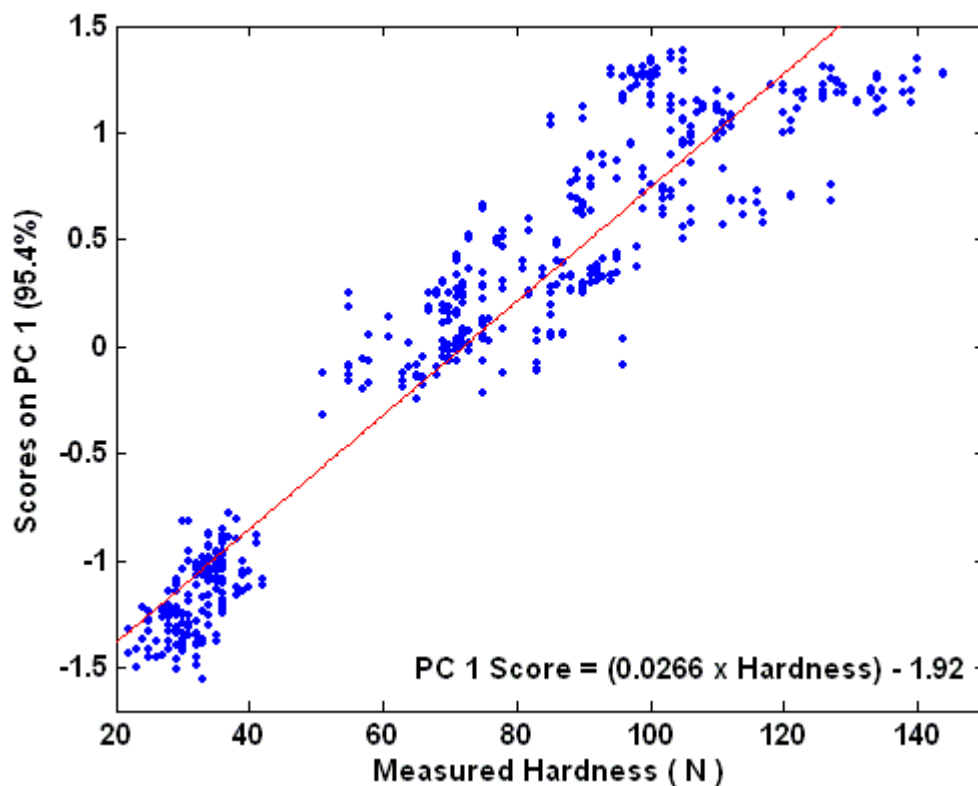


Figure 16. Correlation plot of measured tablet hardness against PC 1 score for compression sample transmittance spectra.

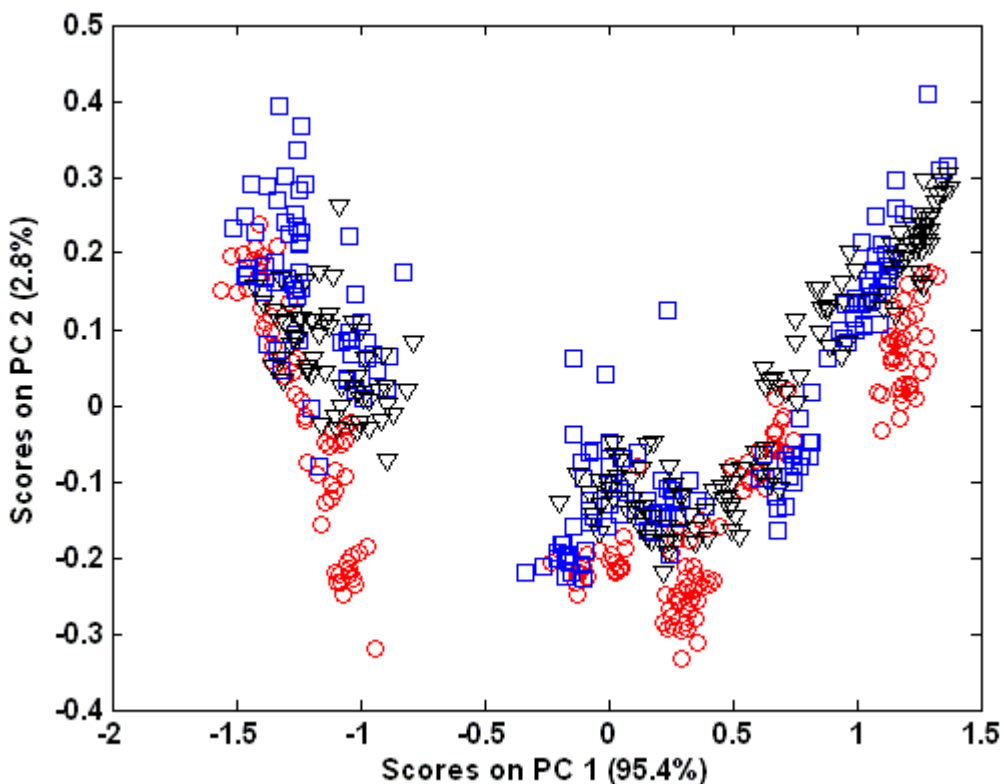


Figure 17. Principal component scores plot from compression sample transmission PCA. Single-punch tablet press = red circles, Small-scale rotary press = blue squares, Large rotary tablet press = black triangles.

### Comparison of Reflection and Transmission Modes

Both the reflection and transmission compression test models demonstrate potential for quantitative predictions. Even though the reflection spectra are sensitive to processing scale, the effect can be included in future models as controlled variation, and will have little effect on the quantitative prediction of other tablet properties. If the hardness models derived during the compression test are applied to the position test spectra, the transmission analyses are affected by positioning error to a much greater extent than the reflection-based analyses, with 3.6 and 2.1 N standard deviation, respectively. Combined with the analyses of the standard deviation of raw and SNV-transformed reflection and transmission spectra discussed earlier (Automatic

Positioning and Shielding Tests), these experiments suggest that reflection measurements are less sensitive to sample positioning error.

## **Conclusion**

The objectives of the work presented here were to:

- I. Qualify capabilities of the instrument and the sample handling system.
- II. Evaluate the potential effect of one source of a process signature on calibration development.
- III. Compare the utility of reflection and transmission data collection methods.

With these objectives in mind, the experimental results presented for these data demonstrate that:

- I. The impact of positioning error on both NIR reflection and transmission analysis can be effectively mitigated using spectral preprocessing techniques, and that the automatic positioning system is sufficiently reliable for general use.
- II. Shielding (or masking) is not required for single-tablet NIR transmission analysis.
- III. Spectra acquired from multiple batches of tablets (production samples), and batches of tablets produced across a range of manufacturing scales (compression samples), can be pooled for quantitative calibration development.
- IV. Diffuse reflection spectra were observed to be less sensitive to sample positioning than transmission spectra.

The conclusions derived from this work were used to guide the collection of a database of NIR tablet spectra. This database was used successfully to develop quantitative calibration models for the prediction of single-tablet potency and hardness. The process of quantitative calibration development and validation is presented in the second installment of this series of papers- "Process Analytical Technology Case Study, Part II: Development and Validation of Quantitative Calibrations for API Content and Tablet Hardness." Subsequently, the third paper in this series, "Process Analytical Technology Case Study, Part III: Method Implementation and Transfer," will present the theoretical and practical aspects of deploying and maintaining NIR calibrations in a validated PAT application.

### **Acknowledgements**

The authors wish to gratefully acknowledge the contributions of Ken Leiper, Benson Associates for his valuable effort in the conception of the work and experimental design used in this and subsequent papers. Additional data collection was performed by Damir Begic. This work was funded through an agreement between DCPT and AstraZeneca.

## References

1. FDA. PAT - A Framework for Innovative Manufacturing and Quality Assurance, Draft Guidance; 2003.
2. FDA. Guidance Documents, Available at: <http://www.fda.gov/cder/guidance/index.htm>. Accessed June 20, 2004.
3. Norris KH, Butler WL. Techniques for obtaining absorption spectra on intact biological samples. *IRE transactions on bio-medical electronics*. Jul 1961;8:153-157.
4. Williams P, Norris K, Editors. *Near-Infrared Technology in the Agricultural and Food Industries, Second Edition*; 2001.
5. Ciurczak EW, Torlini RP, Demkowicz MP. Determination of particle size of pharmaceutical raw materials using near-infrared reflectance spectroscopy. *Spectroscopy (Duluth, MN, United States)*. 1986;1(7):36-39.
6. Shah NK, Gemperline PJ. Combination of the Mahalanobis distance and residual variance pattern recognition techniques for classification of near-infrared reflectance spectra. *Analytical Chemistry*. 1990;62(5):465-470.
7. El-Hagrasy AS, Morris HR, D'Amico F, Lodder RA, Drennen JK, 3rd. Near-infrared spectroscopy and imaging for the monitoring of powder blend homogeneity. *Journal of pharmaceutical sciences*. Sep 2001;90(9):1298-1307.
8. Sekulic SS, Wakeman J, Doherty P, Hailey PA. Automated system for the on-line monitoring of powder blending processes using near-infrared spectroscopy. Part II. Qualitative approaches to blend evaluation. *Journal of pharmaceutical and biomedical analysis*. Sep 1998;17(8):1285-1309.

9. Wargo DJ, Drennen JK. Near-infrared spectroscopic characterization of pharmaceutical powder blends. *Journal of Pharmaceutical and Biomedical Analysis*. 1996;14(11):1415-1423.
10. Rantanen J, Antikainen O, Mannermaa J-P, Yliruusi J. Use of the near-infrared reflectance method for measurement of moisture content during granulation. *Pharmaceutical Development and Technology*. 2000;5(2):209-217.
11. Rantanen J, Jorgensen A, Raesaenen E, et al. Process analysis of fluidized bed granulation. *AAPS PharmSciTech*. 2001;2(4):No pp given.
12. Bijlani VJ, Delado-Lopez M, Adeyeye CM, Drennen JK. Near infrared spectroscopy for monitoring the hardness of roller compaction ribbons. *NIR news*. 2002 2002;13(5):8-14.
13. Morris KR, Stowell JG, Byrn SR, Placette AW, Davis TD, Peck GE. Accelerated fluid bed drying using NIR monitoring and phenomenological modeling. *Drug Development and Industrial Pharmacy*. 2000;26(9):985-988.
14. Ciurczak EW, James K, Drennen I. *Pharmaceutical and Medical Applications of Near-Infrared Spectroscopy*. New York, NY USA: Marcel Dekker, Inc.; 2002.
15. Ciurczak EW. Growth of near-infrared spectroscopy in pharmaceutical and medical sciences. *Proceedings of SPIE-The International Society for Optical Engineering*. 2002;4626(Biomedical Nanotechnology Architectures and Applications):116-125.
16. Brown SD, Sum ST, Despagne F, Lavine BK. Chemometrics. *Analytical Chemistry*. 1996;68(12):21-61.
17. Mobley PR, Kowalski BR, Workman JJ, Jr., Bro R. Review of Chemometrics Applied to Spectroscopy: 1985-95, Part 2. *Applied Spectroscopy Reviews*. 1996;31(4):347-368.

18. Workman JJ, Jr., Mobley PR, Kowalski BR, Bro R. Review of chemometrics applied to spectroscopy: 1985-95, part I. *Applied Spectroscopy Reviews*. 1996;31(1 & 2):73-124.
19. Drennen JK, Lodder RA. Nondestructive near-infrared analysis of intact tablets for determination of degradation products. *Journal of Pharmaceutical Sciences*. 1990;79(7):622-627.
20. Iyer M, Morris HR, Drennen JK, III. Solid dosage form analysis by near infrared spectroscopy: Comparison of reflectance and transmittance measurements including the determination of effective sample mass. *Journal of Near Infrared Spectroscopy*. 2002;10(4):233-245.
21. Kirsch JD, Drennen Jk. Determination of film-coated tablet parameters by near-infrared spectroscopy. *Journal of Pharmaceutical and Biomedical Analysis*. 1995;13(10):1273-1281.
22. Kirsch JD, Drennen JK. Near-infrared spectroscopy: applications in the analysis of tablets and solid pharmaceutical dosage forms. *Applied Spectroscopy Reviews*. 1995;30(3):139-174.
23. Kirsch JD, Drennen JK. Nondestructive tablet hardness testing by near-infrared spectroscopy: a new and robust spectral best-fit algorithm. *Journal of Pharmaceutical and Biomedical Analysis*. 1999;19(3-4):351-362.
24. Ingle JD, Crouch SR. *Spectrochemical Analysis*. Upper Saddle River, NJ USA: Prentice-Hall; 1988.
25. United States Pharmacopeial Convention I. <1119> Near-Infrared Spectrophotometry. *USP-NF, Second Supplement*. Rockville, MD USA: United States Pharmacopeial Convention, Inc.; 2003:3337-3344.

26. Cogdill RP, Anderson CA, Drennen JK. Process Analytical Technology Case Study, Part III: Calibration Monitoring and Transfer. *AAPS PharmSciTech*. 2004;sub.
27. Sparen A, Malm M, Josefson M, Folestad S, Johansson J. Light leakage effects with different sample holder geometries in quantitative near-infrared transmission spectroscopy of pharmaceutical tablets. *Applied Spectroscopy*. 2002;56(5):586-592.
28. ASTM. *International Standard E2363-04 Standard Terminology Relating to Process Analytical Technology in the Pharmaceutical Industry*; 2004.
29. Cogdill RP, Anderson CA, Delgado-Lopez M, et al. Process Analytical Technology Case Study, Part II: Development and Validation of Quantitative for Tablet API Content and Hardness. *AAPS PharmSciTech*. 2004;sub.
30. AACC. "Near-Infrared Methods: Guidelines for Model Development and Maintenance, " AACC Method 39-00. *Approved Methods of the American Association of Cereal Chemists*. 10 ed. St. Paul, MN USA: AACC Press; 1999.

## Tables

## Figure Legends

Figure 1. Wavelength axis accuracy measurement. The center of major peaks in the absorbance spectrum of a wavelength standard (upper curve) are located by calculating the zero crossing of the first derivative (lower curve) of a windowed quadratic fit of the spectrum.

Figure 2. Reflectance linearity testing using certified reflectance standards at 1200 (circles), 1600 (triangles), and 2000 nm (squares).

Figure 3. Single-tablet reflectance spectra with repeated positioning using an automatic tablet transport system. The three irregular spectra are the result of tablet mis-alignment on the transport conveyor belts.

Figure 4. Single-tablet transmission spectra with repeated positioning using an automatic tablet transport system. The four irregular spectra are the result of tablet mis-alignment on the transport conveyor belts.

Figure 5. Production sample reflection spectra after SNV pretreatment (N = 572).

Figure 6. Production sample transmission spectra after SNV pretreatment (N = 572).

Figure 7. Surface plot of the autocorrelation matrix calculated using the raw production sample reflection spectra. The lack of correlation between the major band of variance centered at 1563 nm and any off-diagonal peaks suggests that the variation is not due to chemical changes in the samples, but is more likely an instrumental effect.

Figure 8. First two loading vectors from PCA of production samples and reflection spectrum of pure Lactose. PC 1 (solid line), PC 2 (dashed line), and Lactose (dotted line).

Figure 9. Scores plot of first and second principal components from PCA of production samples using reflection data.

Figure 10. First three loading vectors from PCA of production sample transmission spectra. PC 1 (solid line), PC 2 (dash-dot line), and PC 3 (dotted line).

Figure 11. Scores plot of first three principal components from PCA of transmission spectra of production samples.

Figure 12. First two loading vectors from PCA of reflection spectra from compression samples. PC 1 (solid line), PC 2 (dotted line).

Figure 13. Correlation plot of measured tablet hardness against PC 1 score for compression sample reflectance spectra.

Figure 14. Principal component scores plot from PCA of reflection spectra of compression samples. Single-punch tablet press = red circles, Small-scale rotary press = blue squares, Large rotary tablet press = black triangles.

Figure 15. Score plot of first and second PCs from projection of production sample reflection spectra onto the compression sample model. Note that PC1 correlates well with hardness while PC2 is indicative of process signature.

Figure 16. Correlation plot of measured tablet hardness against PC 1 score for compression sample transmittance spectra.

Figure 17. Principal component scores plot from compression sample transmission PCA. Single-punch tablet press = red circles, Small-scale rotary press = blue squares, Large rotary tablet press = black triangles.